Pressure-induced metallization of the Mott insulator $Fe_XMn_{1-X}S$ system

G.M. Abramova[a,□], A. Hanzawa[b], T. Kagayama[b], Y. Mita[b], E.V. Eremin[a], G.M. Zeer[c], S.M. Zharkov[a,c], S.G. Ovchinnikov[a,c]

[a] Kirensky Institute of Physics, Federal Research Center KSC, Siberian Branch, Russian Academy of Sciences, Krasnoyarsk 660036 Russia [b] KYOKUGEN, Center for Science and Technology under Extreme Conditions, Graduate School of Engineering Science, Osaka University, Toyonaka, Osaka 560-8531, Japan [c] Siberian Federal University, 79 Svobodny pr., Krasnoyarsk 660041, Russia

ARTICLE INFO

Keywords:
Correlated electron systems
Metal-insulator transitions High pressure
and low temperature

ABSTRACT

Electrical resistivity of the $Fe_xMn_{1-x}S$($0 \le X \le 0.29$) single crystals based on the Mott insulator α-MnS is experimentally studied in the temperature range of 2–300 K at ambient pressure (P = 0) and at high (up to 30 GPa) hydrostatic pressures for x = 0.12. The electron subsystem of $Fe_xMn_{1-x}S$ undergoes insulator-to-metal transitions indicated by a resistivity drop by a factor of 10^6 with an increase in the chemical pressure (X) due to the cation substitution under ambient conditions and at the hydrostatic pressure (P_C = 27 ± 5 GPa) for x = 0.12. The results obtained show that the hydrostatic pressure -and cation-substitution induced insulator-tometal transitions in the α-MnS-based Mott compounds have similar mechanisms. The dependence of the critical hydrostatic pressure P_C on the Fe content in $Fe_xMn_{1-x}S$ is established.

1. Introduction

α-MnS has the rock salt structure, similar to that of transition metal monoxides (MnO, FeO, CoO and NiO), which have been in the focus of interest in condensed matter physics for decades as the prototypical examples of Mott insulators [1,2] with the type-II antiferromagnetic (AFM-II) structure [3]. The increased interest in these materials with strong electron correlations is due to the pressure-induced metal-insulator transition accompanied by the loss of the localized magnetic moment [4–7]. One of the discussed mechanisms of the pressure-induced transition from the magnetically ordered to nonmagnetic state is the crossover from the high-to low-spin state at a pressure of about 100 GPa.

MnO with the Neel temperature T_N =122 K and α-MnS with T_N = 150 K are antiferromagnetic ionic crystals, in which the Mn^{2+} ions are localized in the octahedral positions of the NaCl-type structure under ambient conditions (at P = 0) [3]. The electronic energy structures for MnO and MnS are presented in [7,8]. A pressure-induced Mott transition for MnO is observed around 106 GPa [7].

In [9–11], a metal-insulator transition in α-MnS at the pressure of P_C =26–30 GPa at room temperature was revealed by the optical method. At pressures up to 0.6 GPa a α-MnS Neel temperature (T_N) shift from 150 K to room temperature was observed [12]. A spin crossover in α-MnS was found in the range of 30 GPa [10] by the optical method at 300 K.

In this study, we investigate a new $Fe_xMn_{1-x}S$ material synthesized on the basis of α-MnS. Since the radius of the Fe^{2+} ions (0.92 Å) in the high-spin state is smaller than that of the Mn^{2+} ions (0.97 Å), we suggested that the chemical pressure (Fe substitution) in α-MnS affects the physical properties, similar to the hydrostatic pressure. We developed a technique for synthesizing the $Me_xMn_{1-x}S$ (Me = Cr, Fe, Cu) powder and single crystals with $0 < x < 0.3$ [13]. Our preliminary results show that the cation substitution in $Me_xMn_{1-x}S$, similar to the hydrostatic pressure, leads to a decrease in the α-MnS lattice parameter. The fcc unit cell parameter in $Fe_xMn_{1-x}S$ with x = 0.29 at 300 K corresponds to the value observed in α-MnS at a pressure of about 4–5 GPa. With the increasing X in $Fe_xMn_{1-x}S$ the Neel temperature shifts from 150 K to 210 K, and at the pressure up to 4.2 GPa T_N shifts from 205 K to 280 K for x = 0.27 [14].

The $Fe_xMn_{1-x}S$ compounds are of special interest due to different pressure effects on the d^5 and d^6 states. The opposite pressure effects on the effective Hubbard parameter U_{eff} for d^5 and d^6 ions were theoretically determined in [15].

To confirm that the chemical pressure can cause similarly to the hydrostatic pressure, the metallization of α-MnS and to clarify the conductivity mechanism in the α-MnS-based solid solutions, we performed high-pressure and Fe-substitution electrical conductivity experiments on the $Fe_xMn_{1-x}S$ samples.

2. Experimental procedure

The growth of $Fe_xMn_{1-x}S$ single crystals and X-ray diffraction data were described in [13]. The microstructure and elemental composition of a single crystal of $Fe_xMn_{1-x}S$ were investigated by a scanning electron microscope (SEM) JEOL JSM-7001F equipped with an energy dispersive X-ray spectrometer (Oxford Instruments). The resistance measurements were made by a dc four-probe method in the temperature range of 2–350 K on a PPMS facility (Quantum Design, VSA) at the Kirensky Institute of Physics (Krasnoyarsk, Russia) at P = 0. The electrical resistivity under high pressure was measured by the four-probe method at the Osaka University (Toyonaka, Japan) up to 30 GPa using a diamond anvil cell (DAC) [16]. The gold electrodes were put on the sample loaded in the gasket hole and they were buried in NaCl powder of a pressure medium. In other words, the electric probes were pressed directly on the sample by the pressure medium. The wires were insulated from the SUS301 stainless steel gasket by epoxy resin and cubic-BN powder. The pressure was determined by monitoring the fluorescence peak of a small piece of ruby placed inside the DAC.

3. Results and discussion

Fig. 1 shows the SEM images of the single crystal $Fe_xMn_{1-x}S$ with x = 0.1 and x = 0.29.

The results indicate that the crystal consists of the domains with the chemical compositions close to nominal X. Such a domain microstructure is typical for all the investigated single crystals, and the real chemical compositions in the domains may fluctuate in the limit ±

0.02. Since the electrical resistivity is a structurally dependent quantity, the fluctuation of the chemical composition and the formation of the growth regions can affect the value of the resistivity.

Fig. 2 shows the dc resistance of the $Fe_xMn_{1-x}S(0 \le X \le 0.29)$ single crystals in the temperature range of 2–300 K under ambient conditions. In the $Fe_xMn_{1-x}S$ samples with $X < X_C = 0.25 \pm 0.02$,

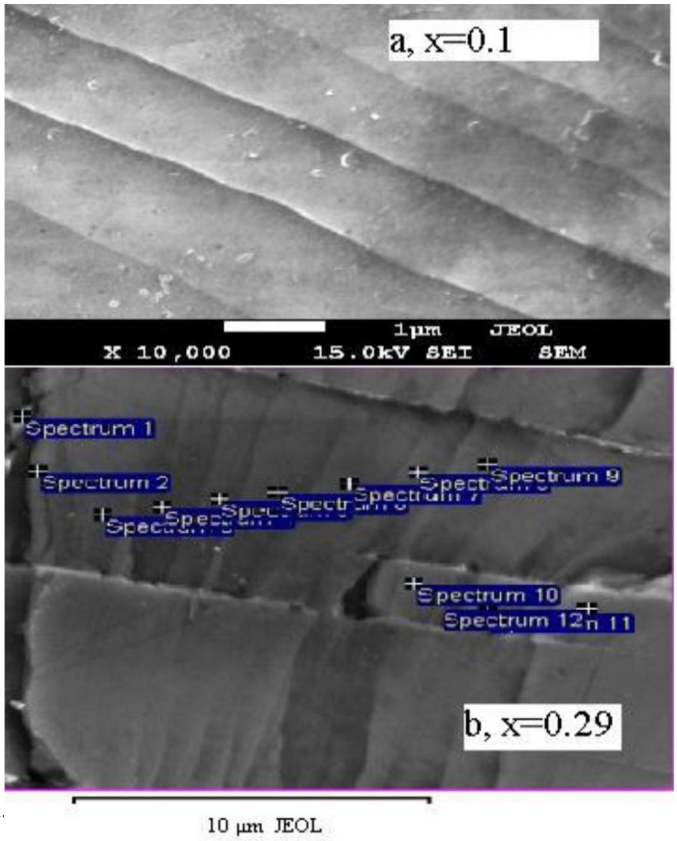

Fig.1.

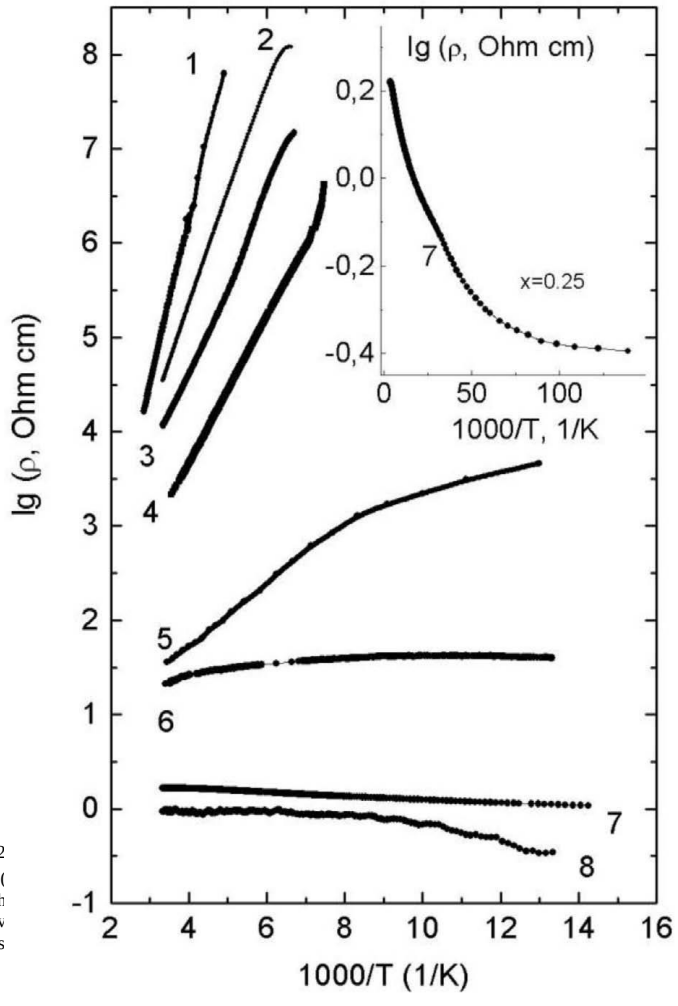

Fig.2 X=0(ert:th sistiv meas

the resistance increases exponentially as the temperature decreases from room temperature. This indicates the thermal activation of the carriers across the energy gap. The thermal energy gap given by logR vs 1/T decreases from 0.37 eV for x = 0 to 0.05 eV for x = 0.21. The resistance of the samples $Fe_xMn_{1-x}S$ with x > 0.21 is not described by the exponential law or the Mott law (at 77–300 K) and then, it has the metallic type of electrical conductivity (Fig. 1, Insert for x = 0.25).

Fig. 3 shows the dependences of the resistivity and thermal activation energy on the unit cell volume of the NaCl lattice type for α-MnS at the pressure up to 5 GPa (the data are obtained based on the results [11]) and for $Fe_xMn_{1-x}S$ at the chemical pressure (X) and under ambient conditions. It can be seen that the cation substitution in α-MnS causes a greater decrease in the electrical resistivity and activation energy for the same decrease in the lattice parameter. Thus, it can be assumed that the value of the electrical resistivity decreases not only due to the lattice compression, but, for example, due to the increase in the electron concentration upon the replacement of $Mn^{2+}(d^5) \rightarrow Fe^{2+}(d^6)$.

Fig. 4 presents the temperature dependences of the resistance (in Ohm) for the $Fe_{0.12}Mn_{0.88}S$ single crystals in the temperature range of 2–300K at different hydrostatic pressures (P).

It can be seen that the temperature coefficient of resistivity is negative at $P \le 26$ GPa, the resistance decreases with the increasing temperature. In the range of 26–27GPa (P_C=27 ± 5GPa) the insulator-to-metal transition in $Fe_{0.12}Mn_{0.88}S$ is observed, and then the resistivity increases with the increasing temperature like in a metal (Insert of Fig. 4). Note that the value of Pc for MnS is 26–30 GPa [9,10].

We did not observe the Mott conductivity with the law $\sigma \sim \exp(T_0/T^n)$, where n = 1/2, 1/3, or 1/4, at low temperatures in the $Fe_xMn_{1-x}S$

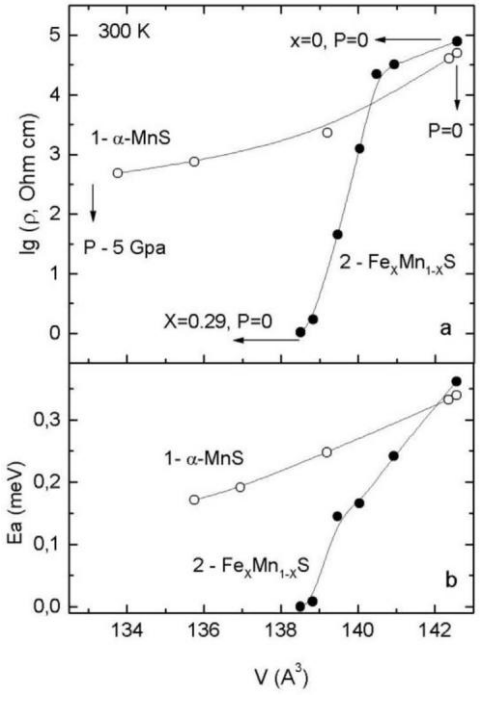

Fig. 3. The volume dependences of the resistivity (a) and the thermal activation gap (b) for α-MnS at the pressure up to 5 GPa (on the basis of data [11]) and for FexMn1–xS at chemical pressure ($0 \le X \le 0.29$) under ambient conditions are presented for comparison.

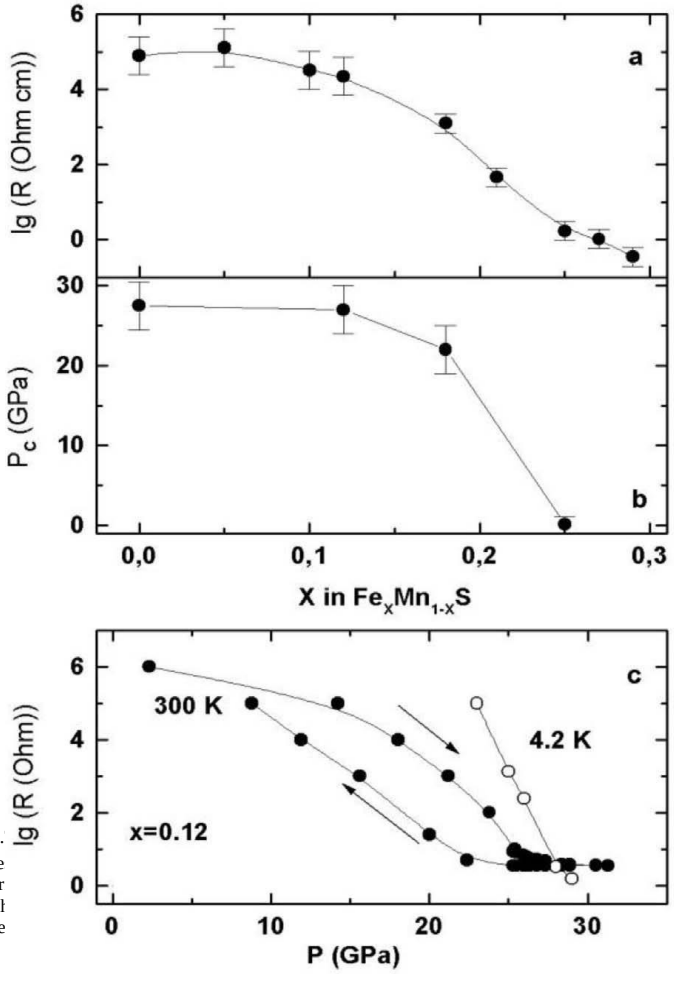

Fig.5. dence Thecr onoftl fthese

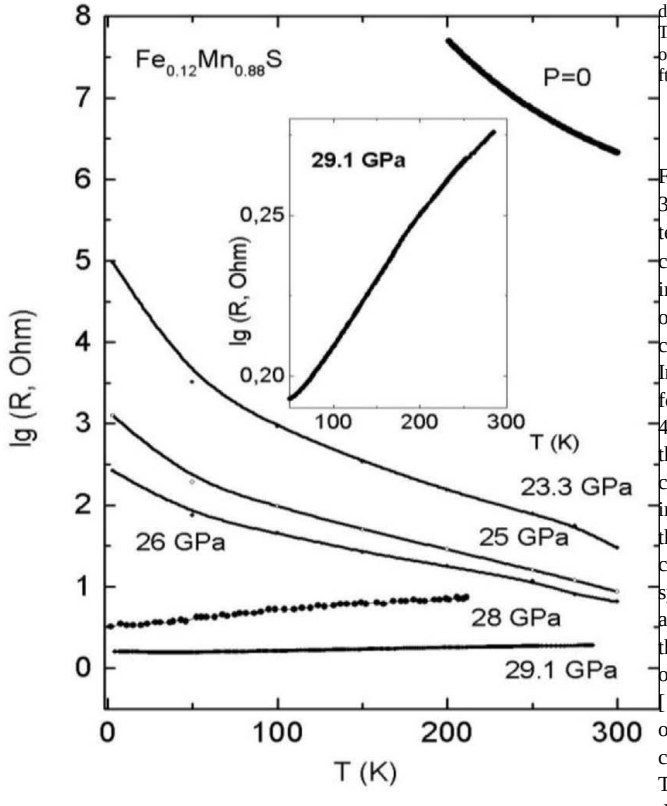

Fig.4.T withX=

semiconductor samples both at the chemical ($x > 0.21$) and hydrostatic pressure (for $x = 0.12$), which is characteristic of the Andersen-type localized state in the energy gap [2]. The thermal activation energy increases non-linearly from zero (around 3–10 K) to 0.05–0.08 eV (around room temperature) for the state at the pressure of 25–26 GPa.

Fig. 5 shows the dc resistance of the FexMn1–xS($0 < X < 0.29$) single crystals at 300 K. For different α-MnS single crystals, the resistivity ρ at room temperature (300 K) is 1.18 10^{4}–10^{5} Ω cm under ambient conditions, which is close to the values reported in [11,17].As the Fe content in FexMn1–xS is increased, the electrical resistance at room temperature decreases by 6 orders of magnitude as compared to that of α-MnS (Fig. 5a) under ambient conditions.

In Fig. 5c, one can see a decrease in the resistance at the hydrostatic pressure for the $Fe_{0.12}Mn_{0.88}S$ single crystals at room temperature and 4.2 K. Hydrostatic compression of the sample produces a gradual decrease in the resistance at room temperature to a value between 10^{6} Ω under ambient conditions (P = 0) and 2 Ω at 29 GPa. A wide hysteresis is observed with the increasing pressure and then removing it (Fig. 5c). The resistance behavior at the hydrostatic pressure is similar to that at the chemical pressure (Fig. 5a and c). The combination of the results indicates that the electrical resistance in the system FexMn1–xS ($0 < X < 0.29$) depends both on the chemical pressure (X) and the hydrostatic pressure (P). The behavior of the electrical conductivity of the FexMn1–xS samples at pressure at room temperature is consistent with the optical gap data at pressures up to 45 GPa ($Fe_{0.18}Mn_{0.82}S$ and $Fe_{0.25}Mn_{0.75}S$ [18,19]). Similar to α-MnS [9],$Fe_{0.18}Mn_{0.82}S$ exhibits a sharp change in the optical reflectance, indicative of the insulator-tometal transition caused by the closing of a dielectric gap with an increase in the pressure up to 22 GPa [19]. The optical reflectance spectra of metallic $Fe_{0.25}Mn_{0.75}S$ at room temperature do not change in the pressure range from 0.1 to 45 GPa [18];at P = 23 GPa its reflectance of this sample is close to that of $Fe_{0.18}Mn_{0.82}S$, which points to a decrease in the optical gap with an increase in the cation substitution degree in FexMn1–xS.

Fig. 5b presents the change of the critical pressure Pc for the transition from the insulator state to the semi-metal state at room temperature with the increasing X. The value of the critical pressure Pc in $Fe_xMn_{1-x}S$ slightly changes in the interval $0 < X < 0.12$ and then decreases. This decrease of Pc is observed in the range of the appearance and growth of the value of the quadrupole splitting in the Mossbauer spectra, which indicates the local distortion of the NaCl-type lattice octahedrons [20]. According to [21] the value of 10Dq in α-MnS increases from 0.9 eV to 1 eV at the pressure up to 5 GPa. Using the results of work [21] we estimated the increase in the crystal field 10Dq with the increasing chemical pressure in $Fe_xMn_{1-x}S$. This estimation indicates that 10Dq increases, at least, up to 0.95 eV with the increasing X in the range of $0 \le X \le 0.29$.

Note, as the value of Pc for $Fe_{0.12}Mn_{0.88}S$ is close to Pc of α-MnS, then the Neel temperature of this sample at P_C can be higher than room temperature, and the low spin state can be formed as in α-MnS [10] at the hydrostatic pressure. While at chemical pressure the Neel temperature of the sample with x = 0.25 is around 200 K [13] under ambient conditions. This fact indicates that the mechanism of changing the magnetic properties $Mn_{1-x}Fe_xS$ can be more sensitive to the change in the interatomic distance.

The obtained results allow one to state the following:

(i) The chemical (under ambient conditions) and hydrostatic pressures lead to similar changes in the resistivity of the Mott compounds $Mn_{1-x}Fe_xS$ based on α-MnS. The insulator-to-metal transition both at the chemical and hydrostatic pressure is accompanied by the narrowing of the energy gap and decreasing of the resistance value.

(ii) The metallization at the chemical and hydrostatic pressures is observed in the entire temperature range of 2–300 K.

(iii) In the $Mn_{1-x}Fe_xS$ sulfides ($x < 0.3$) at room temperature and P = 0, the metallization at the chemical pressure occurs in the Fm–3 m cubic structure without the lattice symmetry transformation.

(iv) The critical hydrostatic pressure P_C of the insulator-to-metal transition depends on the chemical pressure (X) in the solid solutions $Fe_xMn_{1-x}S$ and decreases with increasing concentration of the Fe^{2+} ions from P ≈ 26–30 GPa (for $0 \le X \le 0.12$) to P ≈ 0 (for $x \ge 0.25$).

The origin of the band gaps, the valence and conduction electron states in the 3d-transition-metal compounds were considered by Zaanen, Sawatzky, and Allen (ZSA) in [22,23]. The ZSA diagram of the 3d compounds involves several states. The Mott-Hubbard insulator region corresponds to the insulator state with the energy gap Egap = U, where U is the Coulomb repulsion energy for two electrons at the same atomic site. Holes and electrons move to the d-band with the effective electronic bandwidth W. The Mott localization is expected in narrow band systems when the ratio U/W exceeds the critical value. The next region in the ZSA diagram corresponds to the charge-transfer insulator with Egap = Δ_{CT}, where Δ_{CT} is the charge-transfer energy. The holes are light (anion valence band) and electrons are heavy (d bands). Between these two regions, there is an intermediate one with heavy holes, which corresponds to α-MnS and the transition metal monoxides (MnO, FeO, CoO and NiO) [1].

Fig. 6 presents a schematic band structure of α-MnS at the chemical and hydrostatic pressures without taking into account the structural transition. The lower Hubbard band (LHB) and the upper Hubbard band (UHB) are separated by the effective Mott-Hubbard parameter $U_1 = U_{eff}(d^5) = E_o(d^6) + E_o(d^4) - 2E_o(d^5)$, where $E_o(d^n)$ is the ground term for the d^n configuration. According to [8], U1 = 6 eV for α-MnS. Since the covalence in sulfides is higher than in oxides, the top of the S3p states should be above the LHB top (Fig. 6a). Thus, in the schematic band structure presented in Fig. 6, MnS is the charge-transfer insulator with the direct gap Δ_{ct}. Δ_{ct} =3eV [8]. As the chemical

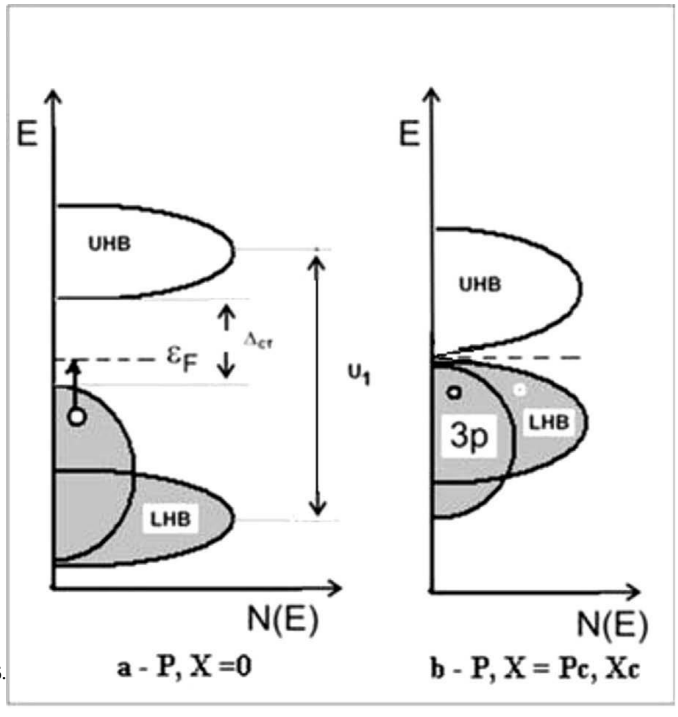

Fig.6.

pressure in $Fe_xMn_{1-x}S$ reduces the lattice parameter, then the effect of X on the electronic structure is similar to the effect of the external pressure. Additionally, the inhomogeneity of the $Fe_xMn_{1-x}S$ electron system ($Mn^{2+}(d^5) \rightarrow Fe^{2+}(d^6)$) increases with the increasing concentration of the additional electron introduced by each atom of iron. The decrease of Pc in $Fe_xMn_{1-x}S$ indicates the decrease of the Hubbard gap U1 with the increase of X, which may be connected with the increasing crystal field value and appearance of the local distortion of the lattice.

At a high pressure, the Hubbard bandwidth W increases, the charge-transfer gap narrows, and at a certain critical pressure P_c metallization occurs (Fig. 6b). The decrease in the nearest neighbor distances of α-MnS with the increasing chemical and hydrostatic pressures can be expected to have the effect of both increasing the amount of the crystal field splitting and increasing the effective (3d) bandwidth W, and additionally decreasing the charge-transfer energy. From here, for understanding the mechanisms of conductivity of the $Fe_xMn_{1-x}S$ samples, the additional investigation of its magnetic properties at pressure is in progress.

4. Summary

The electrical conductivity of the Mott insulator α-MnS-type was studied on the $Fe_xMn_{1-x}S$($0 \le X \le 0.29$) single crystals in the wide temperature range and at the hydrostatic pressures up to 30 GPa. It was found that the resistivity of MnS undergoes a six-order-of-magnitude drop and the conductivity type changes from the semiconductor to metal-type (or semimetal) both at the chemical pressure ($X_C = 0.25$) under ambient conditions and at the hydrostatic pressure with the critical value P_C (x = 0.12). In both cases, at the temperatures of 2–300 K the metallization is observed. The critical hydrostatic pressure P_C decreases with the increasing Fe content in the $Fe_xMn_{1-x}S$ single crystals.

The α-MnS-based compounds can be used for clarifying the mechanism of the Mott metal-insulator transition and the correlation between the electrical and magnetic properties in MnO-type sulfide materials with strong electrons correlations.

Acknowledgment

This study was supported by the KAKENHI JSPS, project no. 18540317.

References

[1] W. Nolting, L. Haunert, G. Borstel, Temperature-dependent electronic structure and magnetic behavior of Mott insulators, Phys. Rev. B 46 (1992) 4426–4431.
[2] N. V. Mott, E.A. Devis. Conduction in non-crystalline systems. Phill. Mag. 17: 1269-1284, 1968; N. F. Mott, E. A. Davis, Electronic Processes in Non-Crystalline Materials. (2nd ed., Clarendon, Oxford, 1979).
[3] J. Corliss, N. Elliot, J. Hasting, Magnetic structures of the polymorphic forms of manganous sulfide, Phys. Rev. 104 (1956) 924–928.
[4] R.E. Cohen, I.I. Mazin, D.G. Isaak, Magnetic collapse in transition metal oxides at high pressure: implications for the earth, Science 275 (1997) 654–657.
[5] I.S. Lyubutin, S.G. Ovchinnikov, A.G. Gavriliuk, V.V. Struzhkin, Spin-crossover-induced Mott transition and the other scenarios of metallization in 3dn metal compounds, Phys. Rev. B 79 (2009) 085125-(1-7).
[6] I.S. Lyubutin, A.G. Gavriliuk, High and ultra-high pressure research on phase transformations in 3d-metal oxides: current progress, Phys.–Uspekhi 52 (10) (2009) 989–1017.
[7] J.R. Patterson, C.M. Aracne, D.D. Jackson, V. Malba, S.T. Weir, P.A. Baker, Y.K. Vohra, Pressure-induced metallization of the Mott insulator MnO, Phys. Rev. B 69 (2004) 220101(R)–220104.
[8] S.J. Youn, B.I. Min, A.J. Freeman, Crossroads electronic structure of MnS, MnSe, and MnTe, Phys. Stat. Sol. (b) 241 (2004) 1411–1414.
[9] Y. Mita, Y. Ishida, M. Kobayashi, S. Endo, S. Mochizuki, Pressure dependence of the optical absorption in alpha-MnS, Phys. B 359–361 (2005) 1192–1194.
[10] Y. Wang, L. Bai, T. Wen, L. Yang, H. Gou, Y. Xiao, P. Chow, M. Pravica, W. Yang, Y. Zhao, Giant pressure-driven lattice collapse coupled with intermetallic bonding and spin-state transition in manganese chalcogenides, Angew. Chem. Int. Ed. 55 (2016) 1–5.
[11] A. Kraft, B. Greuling, High pressure phase transformation in MnS, Crist. Res. Technol. 23 (5) (1988) 605–608.
[12] R. Georges, C.R. Acad. Sci. 268 (16) (1969).
[13] G. Abramova, N. Volkov, G. Petrakovskiy, V. Sokolov, M. Boehm, O. Baukov, A. Vorotynov, A. Bovina, A. Pischjugin, Synthesis and properties of $Mn_{1-x}Fe_xS$ single-crystals at room temperature, J. Mag. Magn. Mat. 320 (2008) 3261–3263.
[14] G. Abramova, M. Boehm, J. Schefer, A. Piovano, G. Zeer, S. Zharkov, Y. Mita, V. Sokolov, Neutron Investigations of the Magnetic Properties of FexMn1−xS under Pressure up to 4.2K, JETP Lett. 106 (8) (2017) 498–502.
[15] S.G. Ovchinnikov, Analysis of the sequence of insulator-metal phase transitions at high pressure in systems with spin crossovers, JETP 116 (2013) 123–127.
[16] M. Kaneshige, S. Hirayama, T. Yabuuchi, T. Matsuoka, K. Shimizu, Y. Mita, H. Hyoudo, K. Kimura, Measurement of electrical resistance and raman spectrum of α-boron under high pressure, J. Phys. Soc. Jpn. 76 (2007) 19–20.
[17] H.H. Heikens, G.A. Wiegers, C.F. Bruggen, On the nature of a new phase transition in α-MnS, Solid State Commun. 24 (3) (1977) 205–209, http://dx.doi.org/10.1016/0038-1098(77)91198-X.
[18] G.M. Abramova, N.V. Volkov, G.A. Petrakovskii, et al., Metal-insulator transition in FexMn1 –xS Crystals, JETP Lett. 86 (2007) 371–374.
[19] Y. Mita, T. Kagayama, G.M. Abramova, G.A. Petrakovskii, V.V. Sokolov, Metallic transition of the colossal magnetoresistance material $Fe_xMn_{1-x}S$(x = 0.18) under high pressure, J. Korean Phys. Soc. 63 (2013) 325–328.
[20] G. Abramova, G.A. Petrakovskii, O.A. Bajukov, et al., Structure and mossbauer studies of manganese monosulfide solid solutions $M_xMn_{1-x}S$(M = Cr, Fe) Phys, Sol. State 52 (2010) 87–91.
[21] M. Kavayahi, T. Nakai, S. Mochizukis, S. Takayamas, Validity of the sugano-tanabe diagram for band states in MnO and MnS under high pressure, J. Phys. Chem. Solids 56 (3–4) (1995) 341–344, http://dx.doi.org/10.1016/0022-3697(94)00205-3.
[22] J. Zaanen, G.A. Sawatzky, J.W. Allen, Phys. Rev. Lett. 55 (1985) 418.
[23] V.I. Anisimov, J. Zaanen, O.K. Andersen, Band theory and Mott insulators: Hubbard U instead of Stoner I, Phys. Rev. B 44 (1991) 943, http://dx.doi.org/10.1103/ PhysRevB.44.943.